Accepted on *Dynamics of Continuous, Discrete and Impulsive Systems*
http://monotone.uwaterloo.ca/∼journal — August 2001

Supervisory Switching Strategy in Motion/Force Control of Robotic Manipulation

D. Prattichizzo[a], D. Borrelli[b] and F. Barbagli[c]

[a]Dipartimento di Ingegneria dell'Informazione
Università degli Studi di Siena, Siena Italy [1]

[b]Officine Galileo
Avionic Systems and Equipment Division (Finmeccanica), Firenze, Italy

[c] Robotics Lab
Stanford University, Palo Alto, CA, USA

Abstract. A switching controller for a class of robotic manipulators with grasping capabilities is presented. The aim is to control the motion of the grasped object along a desired trajectory while complying with contact force constraints. The algorithm successfully performs its control task by switching between several controllers induced by different operating conditions of the manipulator–object system. Simulation results are presented to show the efficacy of the proposed method.

Keywords. General Manipulators, Supervisory Switching Control, Position/Force Control, Nonlinear Dynamics, Linearization.

AMS (MOS) subject classification: 93C10 (Nonlinear systems), 93B18 (Linearization), 93C40 (Adaptive control), 93C85 (robots).

1 Introduction

This paper deals with the position/force control in co–operative robotic manipulation of an object. Often these robotic systems are required to track a desired object trajectory while fulfilling a set of constraints on the contact forces applied to the object, cf. [13].

In the robotics literature the general problem of force/motion control is known as "hybrid control". For a broad overview on this topics the reader is referred to [19] and the references therein. The analysis of the dynamics and the control of manipulation systems becomes more complex when it is not possible to control contact forces in all directions. This usually occurs when the number of DoF's of the robotic device is smaller than the dimension of the contact force space. In [16] such a case has been defined as "defective grasp". This is the norm in industrial applications

[1]Corresponding author: Domenico Prattichizzo, Dipartimento di Ingegneria dell'Informazione, Università degli Studi di Siena. Email: prattichizzo@ing.unisi.it. Fax: +39-0577-233602. Tel: +39-0577-234609. URL: www.dii.unisi.it/∼domenico

where kinematic defectivity is a common factor for almost all grippers. The problem of position/force control for such a wide class of robotic system is the subject of this paper. The dynamics of such a class of systems has been thoroughly described in [16]. The main result of such work consisted in suggesting an organization of the output object–position/contact–force vector, which results functional controllable, exhausts the control capabilities and incorporates the constraints as well as the task requirements for the manipulation system. Such result can be considered as a structural property. Unfortunately, in spite of its generality, the nature of this result is local as it is based on the linearization of the mechanical system dynamics.

The aim of this paper consists in generalizing the results of [16] to the full nonlinear model by means of the logic-based switching technique. A possible approach is to use several different controllers and to switch among them with a logical device according to some performance criterion. If this logic unit, called supervisor, orchestrates the switching between different controllers depending on some input–output observation of the system, then the control algorithm is intrinsically adaptive. This approach, usually referred to as logic-based switching control, has been extensively studied in [3, 7, 8, 9, 11, 12].

The difference of this approach over alternative approaches, as for example the gain-scheduling approach, consists of its ability to select the best controller according to a prediction error minimization rule, instead of by simple inspection of a scheduling variable.

Such techniques have been successfully applied to robotic problems in the past. In [2] authors emphasized the effectiveness of switched control systems with respect to stabilization and performance for redundant manipulators. The idea of using switching control techniques in the adaptive control context to improve tracking performance has been discussed in [15], where switching control is used to select among a set of free parallel running adaptive algorithms. In [6], authors describe a vision-based robot controller which is based on the concepts of dwell–time switching.

In this paper the goal of tracking any given position/force reference trajectory is obtained by selecting in real time the most "appropriate" of a set of prespecified off-the-shelf controllers, built on a set of ad hoc linearized models of the mechanical system. Such controllers are selected according to a model selection rule based on minimization of a performance index, [11]. According to this rule, an "appropriate controller" is placed into the control loop from time to time, in such a way that the output prediction error between the real system output and the output of the model, upon the controller is designed, is minimized. This choice strategy interprets the concept of certainty equivalence [8, 10], and ensures that the controlled system always incorporates a control law based on the model which best reproduces the system behaviour along its trajectory.

The remainder of the paper is organized as follows: Section 2 introduces

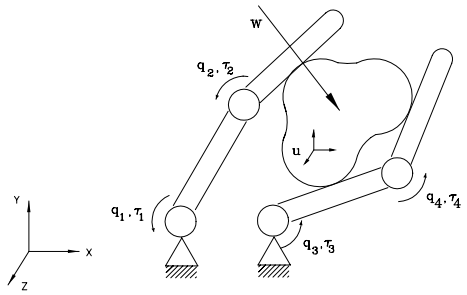

Figure 1: Introducing some notation for a general manipulation system: $\mathbf{q} \in \mathbb{R}^4, \tau \in \mathbb{R}^4, \mathbf{u} \in \mathbb{R}^6, \mathbf{w} \in \mathbb{R}^6$.

the class of manipulation systems for which the force/position control algorithms will be designed. Section 3 introduces the basic concepts of logic–based switching controllers. Section 4 presents in more detail the linear multi input multi output estimator based supervisor which is the core of the logic–based switching controller. Finally Section 5 presents simulation results which prove the concepts previously introduced.

2 General manipulation systems

The class of "general manipulation systems" this paper is concerned with is comprised of mechanisms with any number of limbs (open kinematic chains), of joints (prismatic, rotoidal, spherical, etc.) and of contacts between a reference member called "object" and links in any position of the limb chains, see Fig. 1. This class includes co–operating robots, industrial grippers, robotics hands and so forth, cf. [16, 17, 1] and references therein. As a paradigm for general manipulation systems, we refer to the case of a multi-fingered hand manipulating an object through contacts on its finger parts. An example is reported in Fig. 2

In Section 2.1 the dynamic model for such a class of systems is presented while in section 2.2 previous local results concerning the force/position control for such systems will be reported.

2.1 Linear and non-linear dynamical model

The following notation is used. Refer to Fig. 1, let $\mathbf{q} \in \mathbb{R}^q$ be the vector of joint positions, $\tau \in \mathbb{R}^q$ the vector of joint forces and/or torques, $\mathbf{u} \in \mathbb{R}^d$ the vector locally describing the position and the orientation of a frame attached to the object and $\mathbf{w} \in \mathbb{R}^d$ the vector of external disturbances acting on the object. Finally, introduce the vector $\mathbf{t} \in \mathbb{R}^t$ including forces and torques at

Figure 2: The Barrett Hand mounted on a host arm grasping as electric drill. The hand is a multi–fingered programmable grasper with the dexterity to secure target objects of different sizes, shapes, and orientations. The hand has a low weight (1.18kg) and compact form. *(Courtesy of Barrett Technology Inc.)*

all contacts between the robotic device and the manipulated object.

Assume that contact forces arise from a lumped–parameter model of visco–elastic phenomena at the contacts, summarized by the stiffness matrix $\mathbf{K}$ and the damping matrix $\mathbf{B}$. The Jacobian $\mathbf{J}$ and the grasp matrix $\mathbf{G}$ are defined as usual as the linear maps relating the velocities of the contact points on the links and on the object, to the joint and object velocities, respectively. Note that the visco–elastic contact model is mandatory in all those tasks where contact stiffness is not negligible or in hyperstatic grasps where the rigid–body contact model leaves the dynamics undetermined.

For a complete description of this model, the reader is referred to [16, 17].

The nonlinear dynamics of a general manipulation systems is obtained as

$$\begin{array}{rcl} \ddot{\mathbf{q}} & = & \mathbf{M}_h^{-1}\left(-\mathbf{Q}_h - \mathbf{J}^T\mathbf{t} + \tau\right); \\ \ddot{\mathbf{u}} & = & \mathbf{M}_o^{-1}\left(-\mathbf{Q}_o + \mathbf{G}\mathbf{t} + \mathbf{w}\right); \\ \mathbf{t} & = & \mathbf{K}\mathbf{J}(\mathbf{c}_m - \mathbf{c}_o) + \mathbf{B}\delta(\dot{\mathbf{c}}_m - \dot{\mathbf{c}}_o). \end{array} \tag{1}$$

where $\mathbf{M}_h$ ($\mathbf{M}_o$) is the symmetric and positive definite inertia matrix of the hand (object); $\mathbf{Q}_h$ ($\mathbf{Q}_o$) is the term including velocity–dependent and gravity forces of the hand (object) and $\mathbf{c}_m$ ($\mathbf{c}_o$) is the vector of contact points thought as attached to the hand (object).

In [17, 16], the manipulation system dynamics is linearized at a reference equilibrium configuration

$$\{\tau, [\mathbf{q}, \mathbf{u}, \dot{\mathbf{q}}, \dot{\mathbf{u}}], \mathbf{t}\} = \{\tau_o, [\mathbf{q}_o, \mathbf{u}_o, \mathbf{0}, \mathbf{0}], \mathbf{t}_o\} \tag{2}$$

and in the neighborhood of such an equilibrium, the linearized dynamics of the manipulation system is written as

$$\dot{\mathbf{x}} = \mathbf{A}\mathbf{x} + \mathbf{B}_\tau \tau' + \mathbf{B}_w \mathbf{w}', \tag{3}$$

where state ($\mathbf{x} = \left[(\mathbf{q} - \mathbf{q}_o)^T \ (\mathbf{u} - \mathbf{u}_o)^T \ \dot{\mathbf{q}}^T \ \dot{\mathbf{u}}^T\right]^T$), input ($\tau' = \tau - \mathbf{J}^T \mathbf{t}_o$) and disturbance vectors ($\mathbf{w}' = \mathbf{w} + \mathbf{G}\mathbf{t}_o$) are defined as the departures from the equilibrium configuration.

In [16], it has been shown that a simple PD control of joints variables, asymptotically stabilizes the system in a neighborhood of the equilibrium point. Henceforth the manipulation system will be considered with the PD control and the resulting dynamic matrix of the linearized mode will be indicated as $\mathbf{A}_f$. Note that the input τ' to feedback system $(\mathbf{A}_f, \mathbf{B}_\tau)$ corresponds to the change of the joint references with respect to their equilibria.

2.2 Position/force control and decoupling

One of the main goals of robotic manipulation control is to follow a given trajectory with the manipulated object while guaranteeing that contact forces comply with contact constraints thus ensuring the grasp stability [14, 16]. In the following the position/force controlled outputs will be discussed. The position/force control for robot manipulators with visco–elastic contacts has been investigated in [18, 5]. In those papers the authors consider the position/force control at the end–effector of a single manipulator interacting with a compliant environment.

With reference to object trajectories, rigid–body kinematics play a key role in manipulation control: they do not involve visco–elastic deformations at contacts and can be regarded as low–energy motions. In [17, 1] rigid kinematics were described by the basis matrix Γ whose columns form a basis for $\mathsf{ker}\left[\mathbf{J} \ -\mathbf{G}^T\right] = \mathsf{im}\,(\Gamma) = \mathsf{im}\left[\Gamma_{qc}^T \ \Gamma_{uc}^T\right]^T$ where Γ_{uc} (Γ_{qc}) is a basis matrix of the coordinated rigid–body motions of the object (manipulator) part. Observe that to simplify notation, it is assumed here that $\mathsf{ker}\,(\mathbf{J}) = \{\mathbf{0}\}$ and that $\mathsf{ker}\,(\mathbf{G}^T) = \{\mathbf{0}\}$.

The controlled output vector of object positions is interpreted by the *rigid–body* object motion $\mathbf{u}_c$ defined as the projection of the object displacement $\mathbf{u}$ onto the column space of Γ_{uc}:

$$\begin{aligned} &\mathbf{u}_c = \mathbf{E}_{uc}\mathbf{x}; \quad \text{where} \\ &\mathbf{E}_{uc} = \Gamma_{uc}^T \left[\mathbf{0}\ \mathbf{I}\ \mathbf{0}\ \mathbf{0}\right]. \end{aligned} \tag{4}$$

The second output vector to be controlled consists of internal contact forces. These are self–balanced forces, belong to the null space of the grasp matrix $\mathbf{G}$ and enable the robotic device to grasp the object. In general, not all the internal forces are reachable by control inputs thus we choose as second

controlled output the *reachable internal* contact forces $\mathbf{t}_i$ defined as the projection of the force vector $\mathbf{t}$ onto the null space of $\mathbf{G}$, [16]:

$$\begin{aligned} &\mathbf{t}_i = \mathbf{E}_{ti}\mathbf{x} \quad \text{where} \\ &\mathbf{E}_{ti} = \mathbf{Q}^T\,[\mathbf{Q}\ \mathbf{0}\ \mathbf{Q}\ \mathbf{0}] \quad \text{and} \\ &\mathbf{Q} = (\mathbf{I} - \mathbf{K}\mathbf{G}^T(\mathbf{G}\mathbf{K}\mathbf{G}^T)^{-1}\mathbf{G})\mathbf{K}\mathbf{J} \end{aligned} \tag{5}$$

The following theorem proven in [16], shows that the task–oriented controlled output vector

$$\mathbf{e} = \begin{bmatrix} \mathbf{u}_c \\ \mathbf{t}_i \end{bmatrix} = \mathbf{E}\mathbf{x}; \quad \text{with } \mathbf{E} = \begin{bmatrix} \mathbf{E}_{uc} \\ \mathbf{E}_{ti} \end{bmatrix} \tag{6}$$

exhausts the control capabilities (square system) and is functionally controllable.

Theorem 1 *Under the hypothesis that* $\ker(\mathbf{G}^T) = \mathbf{0}$ *and that* $\ker(\mathbf{J}) = \mathbf{0}$, *the linearized dynamics in Section 2 described by the triple* $(\mathbf{A}_f, \mathbf{B}_\tau, \mathbf{E})$ *is asymptotically stable, square* $(\tau' \in \mathbb{R}^q, \mathbf{e} \in \mathbb{R}^q)$ *and at* $s = 0$, $det(\mathbf{E}(s\mathbf{I} - \mathbf{A}_f)^{-1}\mathbf{B}_\tau) \neq 0$. *This implies the asymptotic reproducibility and functional controllability [4].*

It should be remarked that the first hypothesis in Theorem 1 is structural while the second is technical in nature [16]. The asymptotic reproducibility property of dynamics means that it is possible to asymptotically decouple and track force and position step references by applying the control input

$$\tau = -(\mathbf{E}\mathbf{A}_f^{-1}\mathbf{B}_\tau)^{-1} \begin{bmatrix} \mathbf{u}_{c,ref} \\ \mathbf{t}_{i,ref} \end{bmatrix}. \tag{7}$$

Unfortunately, the open–loop decoupling control (7) is based on the approximate linearized model and thus, as previously mentioned, can only be applied locally around an equilibrium point.

In the rest of the paper an effort is made to recast the problem of position/force control in a logic–based switching framework. The aim is to extend Theorem 1 to the full nonlinear model (1) of general manipulation systems.

3 Logic–based switching framework

The position-force linearized controller is here generalized to the full nonlinear model by means of the logic-based switching technique [3, 8, 9, 11].

It is important to distinguish between the controlled and measured outputs of the system. Let us introduce the measured outputs of the manipulation system consisting of the joint positions and the contact forces in (1)

$$\mathbf{y} = [\mathbf{q}^T, \mathbf{t}^T]^T \tag{8}$$

while the controlled output $\mathbf{e}$ has been defined in (6).

Hence the set of non linear equations modelling the overall system dynamics (1) as well as its outputs, can be rewritten as

$$\begin{array}{l} \dot{\mathbf{x}} = A_M(\mathbf{x}, \tau, \mathbf{w}); \\ \mathbf{y} = C_M(\mathbf{x}); \\ \mathbf{e} = \left[\begin{array}{c} \mathbf{u}_c \\ \mathbf{t}_i \end{array} \right] \end{array} \tag{9}$$

where the state $\mathbf{x} = [\mathbf{q}^T, \dot{\mathbf{q}}^T, \mathbf{u}^T, \dot{\mathbf{u}}^T]^T \in \mathbb{R}^n$ is finite dimensional and $\mathbf{w}$ is the input disturbance.

The *control goal* is to asymptotically track a position/force reference signal $\mathbf{r} = [\mathbf{u}_{c,ref}^T, \mathbf{t}_{i,ref}^T]^T$ by means of a logic–based switching multiestimator and controller. Such unit will have as inputs the joint torques $\tau \in \mathbb{R}^q$ and the measured outputs $\mathbf{y} \in \mathbb{R}^m$ of the robotic nonlinear MIMO system. The basic idea is to divide the state space into a set of equilibrium points, linearize non linear system model for each one of such points and design a control algorithm based on each linear model. These steps are described in Sections 3.1 and 3.2.

Note that, with no loss of generality, from now on assume that $\mathbf{w} = 0$ in (1) and (9).

3.1 Equilibrium points and linearized models

Consider a number N_{eq} of linearized model $(\mathbf{A}_{f,p}, \mathbf{B}_{\tau,p})$, as the ones presented in (3), built around N_{eq} equilibrium points $\left\{\tilde{\tau}_p, \tilde{\mathbf{x}}_p, \tilde{\mathbf{y}}_p\right\}$ $(p = 1, \ldots N_{eq})$ such that

$$A_M(\tilde{\mathbf{x}}_p, \tilde{\tau}_p) = 0; \quad \tilde{\mathbf{y}}_p = C_M(\tilde{\mathbf{x}}_p); \quad \tilde{\mathbf{e}} = [\tilde{\mathbf{u}}_c^T, \tilde{\mathbf{t}}_i^T]^T. \tag{10}$$

For small perturbations around each equilibrium point $\tilde{\mathbf{x}}_p$ the dynamic behaviour of the nonlinear system is modeled as discussed in Section 2:

$$\dot{\delta\mathbf{x}_p} = \mathbf{A}_{f,p}\delta\mathbf{x}_p + \mathbf{B}_{\tau,p}\delta\tau_p, \quad \delta\mathbf{y}_p = \mathbf{C}_p\delta\mathbf{x}_p; \quad \delta\mathbf{e}_p = \mathbf{E}_p\delta\mathbf{x}_p;$$

where $\mathbf{C}_p$ is the Jacobian of C_M in (9) evaluated at the equilibrium point $\mathbf{x}_p$. Henceforth symbol δ will be omitted.

3.2 Closed loop decoupling multicontrollers

The following assumption is one of the keys to the controller design.

Assumption 1 *For control purposes, the behaviour of the control input τ versus the measured output $\mathbf{y}$ of the system in (9) is described with a model $\mathcal{M}$, whereby $\mathcal{M}$ is an unknown member of a suitably defined family $\mathcal{F}_M$ of the type*

$$\mathcal{F}_M = \bigcup_{p \in \mathcal{P}} \mathcal{M}_p \left(1 + \delta\mathcal{M}_p\right) \tag{11}$$

where $\mathcal{M}_p$ are $m \times q$ transfer function matrices indexed by a parameter p belonging to a finite set $\mathcal{P} = \{1, \ldots, N_{eq}\}$. Each family of models of the system is centered about a nominal transfer function matrix $\mathcal{M}_p$, and includes unmodeled perturbation $\delta\mathcal{M}_p$, which take into account the intrinsic nonlinearities of system (9). Moreover let us assume that $\delta\mathcal{M}_p$ is such that for each possible system $\mathcal{M}$ in $\mathcal{F}_M$, there always exists a nominal system model $\mathcal{M}_p$ within the set of models transfer matrices which is 'close' to $\mathcal{M}$ in some suitably defined sense.

Assumption 1 expresses the fact that all the possible dynamic configurations of the robotic manipulation system during its task execution can be 'covered' with an ad hoc chosen set of models $\mathcal{M}_p = \mathbf{C}_p(s\mathbf{I} - \mathbf{A}_{f,p})^{-1}\mathbf{B}_{\tau,p}$, linearized around N_{eq} equilibrium points, plus some relative perturbation $\delta\mathcal{M}_p$ which takes into account the intrinsic unmodeled system nonlinearity.

For each nominal model member $\mathcal{M}_p = \mathbf{C}_p(s\mathbf{I} - \mathbf{A}_{f,p})^{-1}\mathbf{B}_{\tau,p}$ of $\mathcal{F}_M$, it is possible to design a controller $\mathcal{C}_p$ ($p \in \mathcal{P}$) following the guidelines in Section 2.2 so that the feedback interconnection of $\mathcal{M}_p$ with $\mathcal{C}_p$ is asymptotically stable and asymptotically reproducible, i.e. asymptotically decoupled.

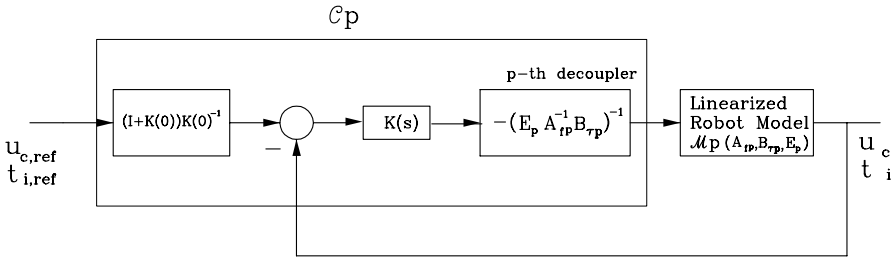

Figure 3: Asymptotic reproducible controller $\mathcal{C}_p$ for linearized model $\mathcal{M}_p$.

The controller $\mathcal{C}_p$ is described in Fig. 3 and consists of

- an open–loop decoupling unit, designed as in (7), which asymptotically decouples the position $\mathbf{u}_c$ and the internal force $\mathbf{t}_i$ outputs for the p–th linearized model $\mathcal{M}_p$;
- a linear controller $K(s)$, with invertible finite gain $K(0)$, stabilizing the closed loop for any linearized dynamics $\mathcal{M}_p$, $p \in \mathcal{P}$;
- a pre–compensator $(I + K(0))K(0)^{-1}$ which is able to compensate the steady state position/force closed–loop error arising when $K(s)$ does not have poles in zero.

It is important to note that, given an equilibrium point of index p, the closed loop controller in Fig. 3 will be able to track step inputs for $\mathbf{u}_c$ and $\mathbf{t}_i$ only in the proximity of such specific state. When this is not the case the

system can switch to the controller designed for the model which is closest to the current state of the system, as suggested in [8, 11]. The unit which is in charge of such commutations will be presented in the following section.

4 Supervisor based on MIMO linear multiestimator

The overall structure is proposed in Fig. 4. The controller is based on two main units: a *multicontroller* structure C_σ and a *linear multiestimator–based supervisory switching logic* $\mathcal{S}$, which are connected in feedback with the robotic system $\mathcal{M}$. Note that the multiestimator ($\mathcal{LEM}_p$) behaviour is affected by the sensed output $\mathbf{y} = [\mathbf{q}^T, \mathbf{t}^T]^T$ and not by the controlled one.

The multicontroller structure will be commanded in such a way that, each controllers of the family will be selected depending on the value of a switching signal σ ($\sigma \in \mathcal{P}$) generated by the logic $\mathcal{S}$. In the following the linear multiestimator system is thoroughly described. Its design follows closely the lines proposed in [11].

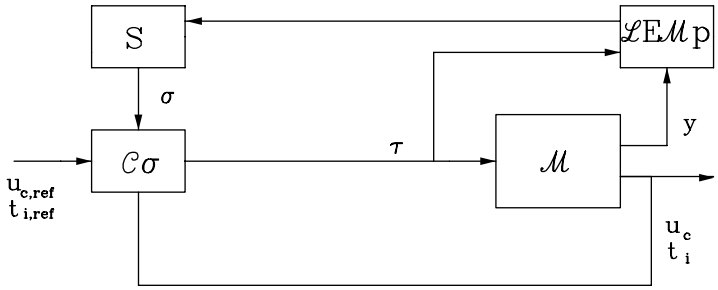

Figure 4: Switching controlled system and robotic manipulation system $\mathcal{M}$.

Let assume to be given the nominal model $m \times q$ transfer matrix $\mathcal{M}_p$, of the p–th linearized model of $\mathcal{M}$:

$$\mathcal{M}_p(s) = \begin{bmatrix} \frac{\beta_p^{11}(s)}{\alpha_p^1(s)} & \cdots & \frac{\beta_p^{1q}(s)}{\alpha_p^1(s)} \\ \vdots & \cdots & \vdots \\ \frac{\beta_p^{m1}(s)}{\alpha_p^m(s)} & \cdots & \frac{\beta_p^{mq}(s)}{\alpha_p^m(s)} \end{bmatrix} \tag{12}$$

where the monic polynomials $\alpha_p^i(s)$ and $\beta_p^{ij}(s)$, $(i = 1, \ldots, m,\ j = 1, \ldots, q,$ $p \in \mathcal{P})$ are the polynomials corresponding respectively, to the denominators and numerators of each row of $\mathcal{M}_p$, and s is the complex variable. The following *linear multiestimator* $\mathcal{LEM}_p$ of $\mathcal{M}_p$ is defined as ($i = 1 \ldots m, \quad p \in$

$\mathcal{P}$)

$$\dot{x}_{E,i} = \tilde{A}_E x_{E,i} + \tilde{G}_E y_i + \tilde{B}_E \begin{bmatrix} \tau_1 \\ \vdots \\ \tau_q \end{bmatrix} \tag{13}$$

$$y_{p,i} = \left[-h^i_{\alpha_p}, h^{i1}_{\beta_p}, \cdots, h^{iq}_{\beta_p}\right] x_{E,i} = c_{p,i}\, x_{E,i} \tag{14}$$

$$e_{p,i} = y_{p,i} - y_i \tag{15}$$

where

$$\tilde{A}_E = \begin{bmatrix} A_E & 0 & \cdots & \cdots & 0 \\ 0 & A_E & 0 & \cdots & 0 \\ \vdots & \vdots & \vdots & \vdots & \vdots \\ 0 & 0 & 0 & 0 & A_E \end{bmatrix}_{\bar{q}\times\bar{q}}, \quad \tilde{G}_E = \begin{bmatrix} b_E \\ 0 \\ \vdots \\ 0 \end{bmatrix}_{\bar{q}\times 1},$$

$$\tilde{B}_E = \begin{bmatrix} 0 & \cdots & \cdots & 0 \\ b_E & 0 & \cdots & 0 \\ 0 & \ddots & 0 & \vdots \\ \vdots & \ddots & b_E & 0 \\ 0 & \cdots & 0 & b_E \end{bmatrix}_{\bar{q}\times q}.$$

The above equations (13)-(15) represent a set of estimators for the i-th component y_i of the sensed robot output $\mathbf{y} = [\mathbf{q}^T, \mathbf{t}^T]^T \in \mathbb{R}^m$. For each fixed $i \in \{1, \ldots, m\}$ all the estimators share the state $x_{E,i}$. In particular, in (13)-(15): p is the model index; $\bar{q} = q + 1$; $i = 1, 2, \ldots, m$ is the row index of $\mathcal{M}_p$; $x_{E,i}$ is a shared state of dimensions $n\bar{q}$, where n is an upper bound on the McMillan degree of all the transfer functions element of $\mathcal{M}_p$, that is, $n > \max_{i,p}\{\deg(\alpha^i_p(s))\}$, $i = 1, \ldots, m$, $p \in \mathcal{P}$; $e_{p,i}$ is the ith component of the output prediction error; A_E is a square $n \times n$ stability matrix such that for any of its eigenvalues λ, it holds that $Re\lambda \leq -\lambda_E < 0$; the couple (A_E, b_E) is controllable, and finally vectors $h^i_{\alpha_p}, h^{ij}_{\beta_p}$, $i = 1, \ldots, m$, $j = 1, \ldots, q$ composing $c_{p,i}$, are obtained from the matrix transfer functions $\mathcal{M}_p$ (12) in such a way that,

$$\left\{\tilde{A}_E + \tilde{G}_E c_{p,i}, \quad \tilde{B}_E, \quad c_{p,i}\right\} \approx \left[\frac{\beta^{i1}_p(s)}{\alpha^i_p(s)}, \ldots, \frac{\beta^{iq}_p(s)}{\alpha^i_p(s)}\right]$$

where by symbol $\approx$ we mean "is a realization of".

The *supervision task* of switching among different controllers is managed by the cascade interconnection of the three subsystems in Fig. 5: the *linear multiestimator* $\mathcal{LEM}_p$ (13)–(15), a *performance signal generator* Π, and a *dwell time switching logic* $\mathcal{S}$.

The *linear multiestimator* produces as outputs a set of local output prediction errors $e_p = y_p - y$, with $e_p \in \mathbb{R}^m$, and $p \in \mathcal{P}$, being $\mathbf{y}$ the measured outputs of the real system and $\mathbf{y}_p$ those of the linearized model $\mathcal{M}_p$. The following remark holds.

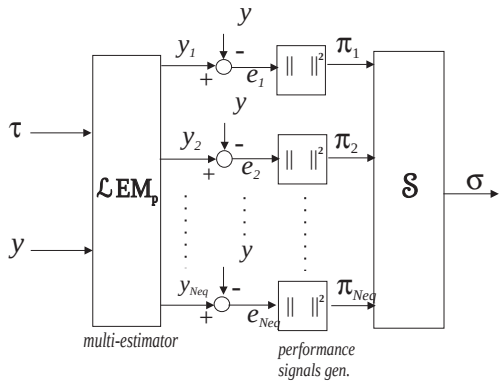

Figure 5: Multiestimator based supervisor.

Remark 1 *The same properties stated for the linear multiestimators presented for example in [11], holds also* locally *for the above linear estimator. In particular, under the feedback interconnection $y = y_p$, $\mathcal{L}E\mathcal{M}_p$ would have to exhibit the same input-output behaviour between τ and y_p as $\mathcal{M}_p$ does between its input and output. This is true since it can be easily proved that, when $y = y_p$, (13),(14) represents an asymptotic realization of the $\mathcal{M}_p$. Therefore, when $\mathcal{M}$ tends to $\mathcal{M}_p$, e_p tends to zero as $e^{-\lambda_E t}$.*

The *performance generator* is a dynamic system with inputs e_p and outputs π_p, which are the the performance signals for each linearized model $\mathcal{M}_p$. Signal π_p is evaluated by integration over time of a measure of the distance between the input–output behaviour of the linearized model $\mathcal{M}_p$, and input–output behaviour of the actual robotic system. Formally, π_p is computed as

$$\dot{\pi}_p(t) = -\lambda\pi_p(t) + \sum_{i=1}^{q} e_{p,i}^2(t), \qquad p \in \mathcal{P}, \quad 0 < \lambda < \lambda_E. \tag{16}$$

The *dwell time switching logic* $\mathcal{S}$ discussed in [11] has been used. It has the role of selecting the controller index σ on the basis of the performance signals π_p of each linearized model by choosing from time to time σ equal to that value of p for which π_p is the smallest. The minimum amount of time that is allowed to elapse between two successive controller switchings is regulated by –that means coincides with– the dwell time τ_D. The dwell time is introduced in order to let the stable dynamics of the closed loop switched system have enough time to decay before the next switching occurs. By doing this the norm of the composite transition matrix is prevented from growing without bounds.

5 Simulation results

An application of the logic–based switching controller to the simple planar (2D) manipulation system of Fig. 6, is reported. The system has

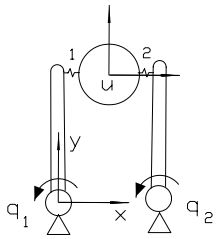

Figure 6: Simple 2–joints, 2–contacts 2D general manipulation system. In this configuration, $q_1 = q_2 = 0$, $\mathbf{u} = [\mathbf{u}_x, \mathbf{u}_y, \theta]^T = [1.5, 3, 0]^T$.

2 joints and 2 contact points, $\mathbf{q} = [q_1, q_2]^T \in \mathbb{R}^2$, $\tau \in \mathbb{R}^2$, $\mathbf{u} = [u_x, u_y, u_\theta]^T \in \mathbb{R}^3$, $\mathbf{t} \in \mathbb{R}^4$. An object with different visco elastic parameters at the contact points is considered. The stiffness matrix is $\mathbf{K} = \text{diag}(\mathbf{K}_1, \mathbf{K}_2), \mathbf{K}_1 = \text{diag}(200N/m, 200N/m)$, $\mathbf{K}_2 = 0.5\mathbf{K}_1$, while the damping one is $\mathbf{B} = \text{diag}(\mathbf{B}_1, \mathbf{B}_2)$, $\mathbf{B}_1 = \text{diag}(66Ns/m, 66Ns/m)$, $\mathbf{B}_2 = 0.5\mathbf{B}_1$; the uniformly distributed link (object) mass and the link length (object radius) are $\mathbf{m}_l = 0.3kg$ ($\mathbf{m}_o = 0.25kg$), $l = 0.3m$ ($R = 0.15m$), respectively. The joint position and velocity (PD) feedback gains are set to $\mathbf{R}_q = \text{diag}(10, 10)$ and $\mathbf{R}_{\dot{q}} = \text{diag}(1, 1)$. The contact point is assumed fixed at a distance $0.9l$ from the joints.

The subspace of rigid–body object motion $\mathsf{im}\,(\Gamma_{uc})$ has dimension 1 thus $\mathbf{u}_c$ in (4) is a scalar output. The same happens for the reachable internal force output $\mathbf{t}_i$ in (5).

As regards reference inputs, a step of 0.5N is commanded to the input $\mathbf{t}_{i,ref}$ corresponding to the internal force with zero initial value. The input $\mathbf{u}_{c,ref}$ corresponding to the rigid–body motion of the object is a sinusoid having frequency 0.8rad/sec., amplitude 15cm and phase $(-\pi/2 - 0.8t_d)$rad with an offset of 15cm. The input reference $\mathbf{u}_{c,ref}(t)$ (dash–dotted line in Fig. 7) is delayed of $t_d = 2$sec with respect to the internal force step.

The robotic system is linearized at three equilibrium points (2) chosen 'close' to the system trajectory corresponding to the commanded object

position inputs, namely

$$\begin{array}{l}\left\{\tilde{\tau}_1^T, [\tilde{\mathbf{q}}^T, \tilde{\mathbf{u}}^T, \tilde{\dot{\mathbf{q}}}^T, \tilde{\dot{\mathbf{u}}}^T]_1, \tilde{\mathbf{y}}_1^T\right\} = \\ \quad \{[0,0], [(0,0)(1.5,3,0)(0,0)(0,0,0)], [0,0,0,0,0,0]\} \\ \left\{\tilde{\tau}_3^T, [\tilde{\mathbf{q}}^T, \tilde{\mathbf{u}}^T, \tilde{\dot{\mathbf{q}}}^T, \tilde{\dot{\mathbf{u}}}^T]_3, \tilde{\mathbf{y}}_3^T\right\} = \\ \quad \{[0,0], [(-\pi/6, -\pi/6)(3, 2.59, 0)(0,0)(0,0,0)], [0,0,0,0,0,0]\} \\ \left\{\tilde{\tau}_2^T, [\tilde{\mathbf{q}}^T, \tilde{\mathbf{u}}^T, \tilde{\dot{\mathbf{q}}}^T, \tilde{\dot{\mathbf{u}}}^T]_2, \tilde{\mathbf{y}}_2^T\right\} = \\ \quad \{[0,0], [(-\pi/3, -\pi/3)(4.1, 1.5, 0)(0,0)(0,0,0)], [0,0,0,0,0,0]\}\end{array}.$$

The linearized models $(\mathbf{A}_{f,p}, \mathbf{B}_{\tau,p}, \mathbf{E}_p)$, $(p = 1, 2, 3;)$, evaluated at the equilibrium points, are used to build the multiestimator. Regarding the multicontroller $\mathcal{C}_p$, the fixed part $K(s)$ in Fig. 3 is a simple proportional controller and is set to $\mathrm{diag}(1, 10)$. Observe that $K(s) = K_0$ stabilizes the linearized models at all the 3 equilibrium points. As regards the multiestimator, the performance generator and the switching logic, we have that the stability margin of A_E is set to $\lambda_E = -1500$; the dynamic behaviour of (16) is set to $\lambda = 100$ and finally the minimum amount of time allowed to elapse between two successive controller switchings (dwell–time) is set to $\tau_D = 0.05$.

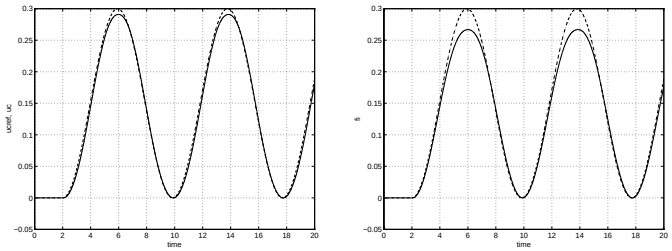

a) b)

Figure 7: Rigid–body object motions starting from the initial configuration in Fig. 6. (a) Logic–based switching control: reference input $\mathbf{u}_{c,ref}$ (dash–dotted line) and system output $\mathbf{u}_c$. (b) Linearized control: reference input $\mathbf{u}_{c,ref}$ (dash–dotted line) and system output $\mathbf{u}_c$.

Simulation results of the switching control technique are compared with those obtained without the switching logic. That is, last results are obtained by the same asymptotically decoupling controller but with the switching variable frozen to $\sigma = 1$ (only the linearization at the first equilibrium point has been considered).

Rigid–body object and internal force trajectories are reported in Fig. 7 and Fig. 8, respectively. Note that the outputs of the switching adaptive system follow their references, in spite of the persistence of the variation of the reference input in Fig. 7–a.

In Fig. 9 the plot of switching variable σ has been reported together with joint variable $q_1(t)$.

By simple inspection, it clearly appears that the switching logic increases the system performances in position and force tracking.

Observe that the nonlinear system does not pass through the equilibrium points employed to compute the linearized models. This is mainly due to the continuous variations of position inputs and to the fact that the internal force is zero at all the equilibrium points.

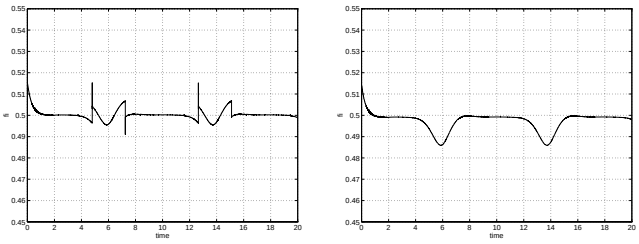

a) b)

Figure 8: Reachable internal force behaviour when the reference input is a step of 0.5N. To the initial configuration (Fig. 6), It corresponds a zero internal force. (a) Logic–based switching. (b) Linearized control with $\sigma = 1$.

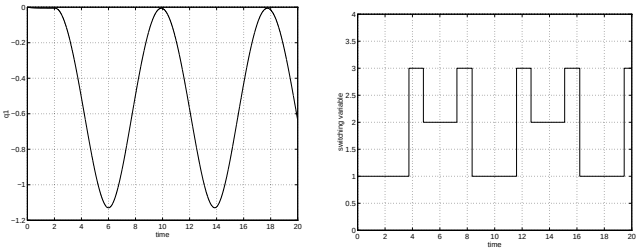

a) b)

Figure 9: In Fig. a) it is reported the plot of the first joint variable $q_1(t)$ while in Fig. b) it is reported the plot of the switching variable σ. Note that to $q_1 = 0$ ($q_1 = -\pi/6$) $\{q_1 = -\pi./3\}$, it corresponds a linearized model with $\sigma = 1$ ($\sigma = 3$) $\{\sigma = 2\}$.

It is worth stressing that in this section, for the sake of brevity, we have assumed to possess an exact knowledge of the system model on which it is based the decoupling control in Fig. 3. Normally, this is not the case and parameter uncertainties should be considered. Observe that taking into account uncertainties is an easy matter in the framework of the multiestimator–based switching control, [11].

6 Conclusions

This paper analyzes the problem of controlling motions of objects manipulated by multiple robotic limbs, taking into account the possibility of kinematic defectivity of the mechanism and the fact that friction imposes constraints on permissible contact forces, and therefore requires planning of force trajectories together with position trajectories. The paper define the controlled outputs which incorporate the constraints as well as the task requirements for the system in terms of forces and manipulated object trajectories.

The proposed position/force controller is based on linearized dynamics and works for a wide class of manipulation systems referred to as "general manipulation systems". The problem of generalizing the local result to the full nonlinear model has been approached in a logic–based switching framework. A logic–based switching controller has been developed for the full nonlinear manipulation system dynamics. Its performance is successfully shown via simulations. The multicontroller switches among several controllers designed for linear approximation of the robotics nonlinear dynamics. The aim is to obtain an asymptotic tracking of the object motion and internal force in a co–operative grasp of a single object.

The main contribution and motivation of this work consists in using the logic–based switching control to steer the nonlinear dynamics of general manipulation systems through 'local' controllers with no known global properties. An important issue that must be settled to synthesize the proposed logic–based switching control is the choice of the equilibrium points. At this stage of the work we simply select a set of equilibrium points 'close' to the nominal trajectory. Further investigation is needed to address some criterion of optimality in choosing the linearized models. Currently the research is addressed towards the systematic investigation of the full characterization of the system salient global properties.

References

[1] A. Bicchi, D. Prattichizzo, "Manipulability of Cooperating Robots with Unactuated Joints and Closed–Chain Mechanisms," *IEEE Transactions on Robotics and Automation*. Vol. 16. No. 4. pp. 336–345. Aug. 2000.

[2] B.E. Bishop, M.W. Spong, "Control of redundant manipulators using logic–based switching," in *Proc. Conf. on Decision and Control*, Tampa, Florida, Dec. 1998.

[3] D. Borrelli, A. S. Morse and E. Mosca "Discrete-time supervisory control of families of two-degrees-of-freedom linear set-point controllers," in *IEEE Trans. Automat. Contr.*, Vol. 44, No.1, pp. 178–181, Jan. 1999.

[4] R.W. Brockett, M. Mesarovich, "The Reproducibility of Multivariable Systems," in *Jour. Math. Anal. Appl.,* vol. 11, 584–563, 1965.

[5] S. Chiaverini, B. Siciliano, L. Villani, "An adaptive force/position control scheme for robot manipulators," *Applied Mathematics and Computer Science*, 7, 293-303, 1997.

[6] W.C. Chang, A. S. Morse, G. D. Hager, "A Calibration-Free, Self-Adjusting Stereo Visual Control System," in *Proc. of IFAC World Congress*, S. Francico,California, June 1996.

[7] J. Hespanha and A.S. Morse, "Supervision of Families of Nonlinear Controller", In *Proc. of the 35th Conf. on Decision and Contr.*, pagg. 3772-3773, Dec. 1996.

[8] J. Hespanha and A.S. Morse, " Certainty equivalence implies detectability". *System & Control Letters*, 36(1):1-13, Jan. 1999.

[9] J. Hespanha and D. Liberzon and A. S. Morse. "Bounds on the Number of Switchings with Scale-Independent Hysteresis: Applications to Supervisory Control," in *Proc. of the 39th Conf. on Decision and Contr.*, Dec. 2000."

[10] S.R. Kulkarni and P.J. Ramadge, "Model and controller selection policies based on output prediction errors," in *IEEE Trans. Automat. Contr.*, Vol. 41, No.11, Nov. 1996.

[11] A. S. Morse. "Supervisory control of families of linear set-point controllers: part 1, exact matching," in *IEEE Trans. Automat. Contr.*, Vol. 31, N.10, pp. 1413–1431, 1996.

[12] A. S. Morse. "Supervisory control of families of linear set-point controllers: part 2 - robustness," *IEEE Trans. Automat. Contr.*, Vol. 42, No.11, pp. 1500–1515, Nov. 1997.

[13] R.M. Murray, Z. Li e S.S. Sastry, *A mathematical introduction to robotic manipulation*, Boca Raton, Florida, CRC Press, 1994.

[14] Y. Nakamura, K. Nagai, T. Yoshikawa, "Dynamics and stability of multiple robot mechanisms," in *Int. Journal of Robotics Research*, Vol.8, No.2, April 1989.

[15] K.S. Narendra and J. Balakrishnan, "Adaptive control using multiple models," *IEEE Trans Automat. Contr.*, Vol. 42, No. 2, pp. 171–187, Feb. 1997.

[16] D. Prattichizzo and A. Bicchi. "Consistent task specification for manipulation systems with general dynamics," *ASME J. Dyn. Sys. Meas. Control*, pp. 760–767 Dec. 1997. An extended report is available at www.dii.unisi.it/∼domenico

[17] D. Prattichizzo and A. Bicchi. "Dynamic analysis of mobility and graspability of general manipulation systems," *IEEE Trans. Rob. Aut.*, Vol. 14, No.1, pp. 1–18, 1998.

[18] B. Siciliano, L. Villani, "An output feedback parallel force/position regulator for a robot manipulator in contact with a compliant environment," *Systems & Control Letters*, 29, 295-300, 1997.

[19] B. Siciliano, L. Villani, *Robot Force Control*, Kluwer Academic Publishers, Boston, MA, 1999